New approximate phase functions:
test for nonspherical particles

S.K. Sharma[a,*], A.K. Roy[b]

[a]S N Bose National Centre for Basic Sciences, Block JD, Sector III, Salt Lake, Calcutta-700 091, India
[b]Physics and Applied Mathematics Unit, Indian Statistical Institute, 203, B T Road, Calcutta-700 035, India

Abstract

In a recent paper, we described two approximate phase functions for the scattering of light by monodisperse particles. One phase function for particles of size small or comparable to the wavelength of scattering radiation and the other for larger particles. Validity of these phase functions was established by comparing their predictions against Mie phase functions. In this paper we examine the validity of these phase functions for monodisperse aligned nonspherical particles. The nonspherical particles employed for examining approximate phase functions are spheroids and infinitely long cylinders. Results show that the predictions of our approximate phase functions are equally valid for nonspherical particles too.

1. Introduction

An important concept in multiple scattering problems is the single-scattering phase function. The exact phase function is determined by the scattering quantities obtained from the solutions of Maxwell equations for the scattering of light by a single scatterer, the size distribution of the scatterers and also by the orientation in case of nonspherical scatterers. No wonder, the exact description of the phase function is very complex in nature. This complexity of exact single-scattering phase functions has led to designing of simple and accurate approximate phase functions which would simplify the solution of the multiple scattering problem. Quite a number of approximate

phase functions have thus been developed. Some of the commonly used models for the phase functions are the Henyey Greenstein [1] phase function, Legendre polynomial decomposition functions [2], the three-parameter phase function [3,4], the two-parameter phase function [5], the Liu phase function [6] etc. However, search for more useful approximate phase functions still continues.

In a recent paper [7] we proposed two new approximate phase functions: one for particles of sizes small or comparable to the wavelength of the scattering radiation and the other for larger particles. These phase functions were tested numerically against exact results for monodispersions of spherical particles of various sizes. The Henyey–Greenstein and the Liu phase functions were also included in this comparison. The small particle approximate phase function of ours was found to be nearly as good as the exact phase function itself. For large particles, the new phase function of ours, although not as good as the corresponding one for small particles, was noted to be better than other approximate phase functions.

A natural question that concerns us is how good are these phase functions in point of applicability in the cases of various kinds of nonspherical particles? In this paper, we attempt to answer this question by numerical comparisons of exact and approximate phase functions for nonspherical particles. For this purpose, as the first case, we examine the accuracy of the new phase functions for the scattering of light by spheroidal particles. The second case for which we examine the new phase functions is the scattering of light by infinitely long cylinders. In both cases we limit ourselves to the scattering of unpolarized light by aligned monodisperse homogeneous dielectric scatterers. The model of scattering by infinitely long cylinders is a widely employed model in atmospheric optics. This scattering model corresponds to two-dimensional scattering geometry and hence the phase functions constructed for the three-dimensional geometry need to be appropriately modified for being applicable to this case. Thereby, we obtain analogues of the new phase functions for the scattering of light by infinitely long cylinders. Although we have limited our present study to monodisperse aligned scatterers, we note that the proposed approximate formulae are expected to work equally well for polydisperse and nonaligned particles too.

We have organized this paper as follows. In Section 2 we digress the relevant formulae from our earlier work [7]. Section 3 gives an account of the test of these phase functions for spheroidal particles. In Section 4, we obtain expressions for new phase functions for infinitely long cylinders and examine their validity against the exact results. Finally, in Section 5, we conclude by summarizing our results.

2. Relevant formulae

For small particles, ($x \leq 1$, where $x = \pi d/\lambda$ is the size parameter with d as the characteristic dimension of the scatterer and λ as the wavelength of the scattering radiation), the new phase function [7] reads as

$$\Phi^s_{new} = a_0 + a_1 \cos\theta + a_2 \cos^2\theta + a_3 \cos^3\theta + a_4 \cos^4\theta, \tag{1}$$

where

$$a_0 = \Phi_{ex}(\pi/2), \qquad a_1 = \frac{d\Phi_{ex}}{d(\cos\theta)}\bigg|_{\theta = \pi/2},$$

$$a_2 = \frac{15}{8\pi} - \frac{3}{4}[\Phi_{ex}(0) + \Phi_{ex}(\pi) + 8\Phi_{ex}(\pi/2)],$$

$$a_3 = \frac{\Phi_{ex}(0) - \Phi_{ex}(\pi)}{2} - a_1,$$

and

$$a_4 = \frac{5}{4}[\Phi_{ex}(0) + \Phi_{ex}(\pi) + 4\Phi_{ex}(\pi/2)] - \frac{15}{8\pi}.$$

Here Φ_{ex} refers to the exact phase function. The constraints used in arriving at the expressions for $a_0 \ldots a_4$ are: (i) The Φ^s_{new} in spherical geometry is normalized according to the relation

$$2\pi \int_{-1}^{1} \Phi^s_{new}(\cos\theta)\, d(\cos\theta) = 1.$$

(ii) The new phase function Φ^s_{new} matches with Φ_{ex} at $\theta = 0$, $\pi/2$, and π. (iii) The slope of Φ^s_{new} is identical with that of Φ_{ex} at $\theta = \pi/2$.

The phase function Φ^s_{new} given by (1) can also be expressed in a more familiar form:

$$\Phi^s_{new} = b_0 + b_1 P_1(\cos\theta) + b_2 P_2(\cos\theta) + b_3 P_3(\cos\theta) + b_4 P_4(\cos\theta),$$

where, comparing it with (1), the coefficients $b_0, b_1, \ldots, b_4$ can be easily identified as

$$b_0 = a_0 + \tfrac{1}{3}a_2 + \tfrac{1}{5}a_4, \qquad b_1 = a_1 + \tfrac{3}{5}a_3,$$

$$b_2 = \tfrac{2}{3}a_2 + \tfrac{4}{7}a_4, \qquad b_3 = \tfrac{2}{5}a_3, \qquad b_4 = \tfrac{4}{35}a_4.$$

It may also be mentioned here that since Eq. (1) contains even as well as odd powers of $\cos\theta$, positivity of the phase function is not guaranteed in (1). Although, in all the test cases examined, which include spherical as well as nonspherical particles, we find that the phase function remains positive as long as the sizes of the scattering particles are small in comparison to the scattering radiation, a formal proof could not be obtained.

For large particles ($x \geq 3$), the new phase function reads as

$$\Phi^l_{new} = \left[\frac{(\cos\theta)^{2\mu} + (\cos\theta)^{2\nu+1}}{2}\right]\Phi_{ex}(0) + (1 + \cos\theta)^p (1 - \cos\theta)^q \Phi_{ex}(\pi/2)$$

$$+ (\cos\theta)^{2k}\frac{1 - \cos\theta}{2}\Phi_{ex}(\pi) + s_1 \cos^2\theta(1 - \cos^2\theta) + s_2 \cos^3\theta(1 - \cos^2\theta). \qquad (2)$$

In (2), the indices μ, ν and k are positive integers such that $\nu \geq \mu$. The indices p, q are positive numbers. It may be noted that the phase function (2) is so constructed that it coincides with the exact phase function at $\theta = 0$, $\pi/2$ and π. The first three terms on the right-hand side of (2) in fact determine the behaviour of the phase function in the near forward, around $\theta = \pi/2$ and in the backward directions, respectively. In the second term, the parameters p and q generate the required asymmetry around $\theta = \pi/2$. The fourth and fifth terms on the right-hand side of (2) actually ensure the correct normalization of the phase function and the correct reproduction of the asymmetry

parameter, respectively. We note here that with Φ^l_{new} given by (2), the multiple scattering integral appearing in the radiative transfer equation can be evaluated analytically. Also the problem of determination of cutoff value when the phase function is expressed as Legendre polynomial decomposition does not crop up here.

The parameters in (2) are obtained by employing the following relations:

$$a_{pq}\Phi_{ex}(\pi/2) + \frac{1}{2\mu + 1}\Phi_{ex}(0) + \frac{1}{2k + 1}\Phi_{ex}(\pi) + \frac{4}{15}s_1 = \frac{1}{2\pi}, \tag{3}$$

$$b_{pq}\Phi_{ex}(\pi/2) + \frac{1}{2v + 3}\Phi_{ex}(0) - \frac{1}{2k + 3}\Phi_{ex}(\pi) + \frac{4}{35}s_2 = \frac{g}{2\pi}, \tag{4}$$

where

$$a_{pq} = \int_{-1}^{1} (1 + \cos\theta)^p(1 - \cos\theta)^q \, d(\cos\theta),$$

$$b_{pq} = \int_{-1}^{1} \cos\theta(1 + \cos\theta)^p(1 - \cos\theta)^q \, d(\cos\theta),$$

and g is the asymmetry parameter. Eq. (3) results from the normalization requirement whereas Eq. (4) results from the requirement that Φ^l_{new} reproduces the correct value of g. To obtain the desired parametrization of the phase function, we adjust the parameters μ, v, p, q and k in a manner so that s_1 and s_2 are reduced to as small numbers as possible. This is required to ensure that the phase function given by (2) remains positive for all θ values. The structure of terms $s_1 \cos^2\theta(1 - \cos^2\theta)$ and $s_2 \cos^3\theta(1 - \cos^2\theta)$ tells us that if $s_1 \sim s_2$ and both are positive and small then as $s_1 \cos^2\theta(1 - \cos^2\theta) > s_2 \cos^3\theta(1 - \cos^2\theta)$ for all θ, one does not encounter much difficulty in ensuring positive definiteness of expression (2). Problem may occur if s_1 is negative or if s_2 is much greater than s_1. Once a few cases are worked at, it becomes clear as to how to adjust s_1, s_2 so that the values of s_1, s_2 remain within the desired range. Although, we have restricted ourselves to integral p, q values, the use of nonintegral values is also permitted and may yield even better results. For lower x values in the domain of applicability of Φ^l_{new}, a variant of it, namely, Φ^{ls}_{new} [7], which employs the term $\cos^{2\mu}\theta((1 + \cos\theta)/2)^2\Phi_{ex}(0)$ in place of the first term on right-hand side of (2) keeping all other terms intact, was found to be very useful and more appropriate as an approximation to the exact phase function. This would, however, result in replacing the factor $1/(1 + 2\mu)$ in Eq. (3) by $\frac{1}{2}[1/(1 + 2\mu) + 1/(3 + 2\mu)]$ and putting $v = \mu$ in Eq. (4).

The phase functions (1) and (2) were examined [7] for monodispersions of Mie particles of various sizes. It was found that (1) is capable of reproducing the exact phase function truly and completely at all scattering angles when $x \leq 1$. The formula works pretty well upto $x \leq 2$ and reasonably well for $x \leq 3$. For large particles, the phase function Φ^l_{new} given by (2) and its variant Φ^{ls}_{new} constitute significant improvement over the Henyey–Greenstein phase function in the forward lobe. In addition, it appears to be a better representation of true phase function in comparison to the Henyey–Greenstein phase function away from the forward lobe too.

3. Test of new phase functions for spheroidal particles

In this section we present numerical comparison of the new phase functions with exact phase functions for the scattering of light by a monodispersion of aligned spheroidal particles. Prolate as well as oblate spheroids have been considered. The exact phase functions have been obtained by employing a computer program for the scattering quantities of a spheroid given by Barber and Hill [8]. To make the comparisons more meaningful, we have also included in this comparison, the most widely used approximate phase function, namely, the Henyey–Greenstein phase function.

The description of scattering function for spheroidal particles remains essentially similar to the case of spherical particles. This means that the functions Φ^s_{new}, $\Phi^l_{new}(\Phi^{ls}_{new})$ and all the associated analysis done in the context of spherical particles could be applied to the case of spheroidal geometry as well. Thus, Eqs. (1)–(4) and all the associated quantities defined in Section 2 are valid and get meaningfully extended to the case of spheroidal particles in a natural way.

Figs. 1–3 show comparisons of Φ^s_{new} with Φ_{hg} and Φ_{ex} for prolate spheroids of $x = 0.1, 0.5$ and 1.0, respectively. Here, $x = 2\pi a/\lambda$, $2a$ being the dimension of a spheroid along the symmetry axis. In all these comparisons, the refractive index, m, is 1.5 and the axial ratio, a/b, has been taken to be 2.0. Evidently, $2b$ is the diameter of the equatorial circle. The subscript hg refers to Henyey–Greenstein and the Φ_{hg} has the expression

$$\Phi_{hg} = \frac{1 - g^2}{4\pi(1 + g^2 - 2g\cos\theta)^{3/2}}. \tag{5}$$

It is clear from these figures that whereas Φ^s_{new} nearly overlaps with the exact phase function, Φ_{hg} does not constitute a good approximation. The results are very similar for oblate spheroids. This can be seen in Fig. 4 where we have compared the exact and approximate phase functions for $x = 1.0$ with $m = 1.5$ and $a/b = 0.4$.
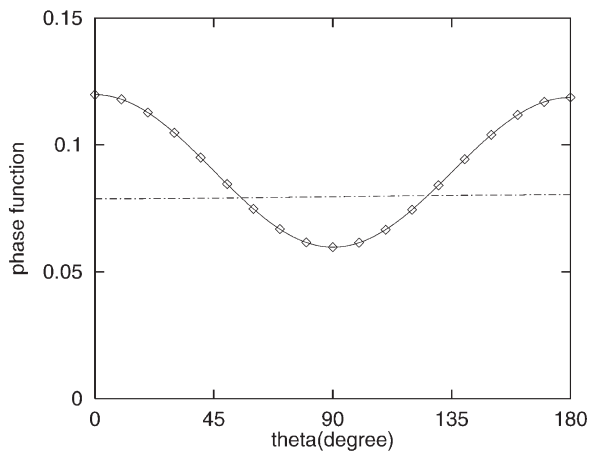

Fig. 1. A comparison of $\Phi^s_{new}(\theta)$ with $\Phi_{ex}(\theta)$ for aligned monodisperse spheroidal particles. Here $x = 0.1$, $m = 1.5$ and $a/b = 2.0$. Solid line: $\Phi_{ex}(\theta)$; Boxes: $\Phi^s_{new}(\theta)$; Dash-dot line: $\Phi_{hg}(\theta)$.
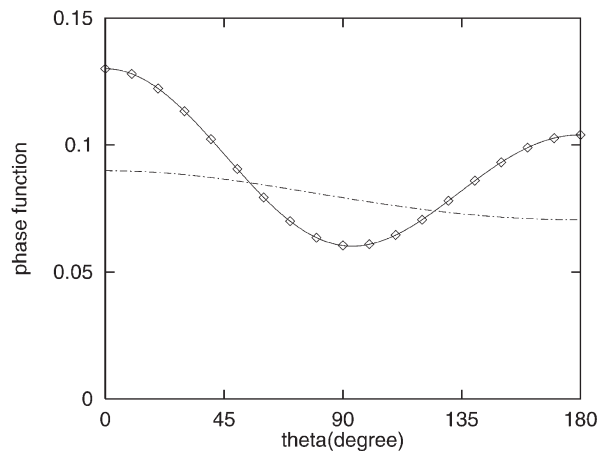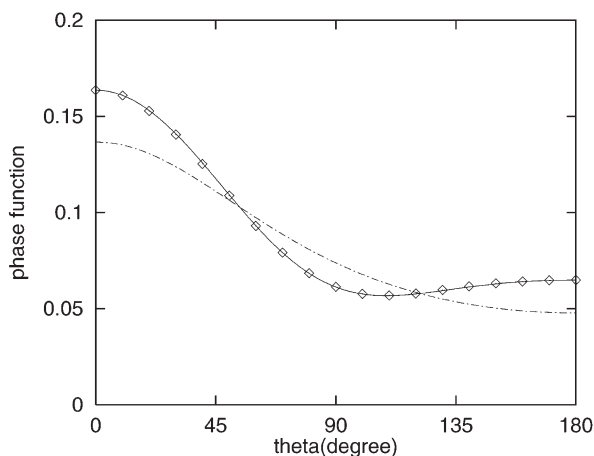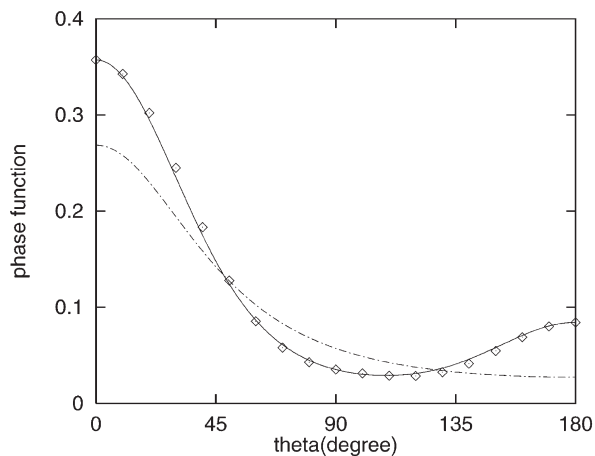
Fig. 2. Same as Fig. 1, but with $x = 0.5$.

Fig. 3. Same as Fig. 1, but with $x = 1.0$.

Fig. 4. Same as Fig. 3, but with $a/b = 0.4$.

Comparisons of the exact and approximate phase functions for large prolate spheroidal particles have been shown in Figs. 5 and 6 for $x = 5.0$ and 10.0, respectively. For these cases also, we have, $m = 1.5$ and $a/b = 2.0$. The maximum size parameter for which the numerical results are convergent and hence meaningfully obtained using the computer program of Barber and Hill is about 12.7 for $a/b = 2.0$ [8]. For this reason, we have restricted our investigation to a maximum value of $x = 10.0$. It is clear from these comparisons that $\Phi^{l}_{new}(\Phi^{ls}_{new})$ are better representations of the exact phase function for large spheroids in comparison with the Henyey–Greenstein phase function. The values of various parameters corresponding to graphs in Figs. 5 and 6 are shown in Table 1.

For spheroids oriented randomly in three dimensions, the phase function can be obtained by placing the particle in many fixed orientations and integrating the scattering quantities over the different orientations. Barber and Hill [8] have examined the effect of random orientations for spheroids of $x = 5.0$ with $a/b = 2.0$ and $m = 1.68 + i0.0001$. As expected, the oscillations in the angular variation of the phase function diminish and shape of the phase function is somewhat similar to that of small particle phase function. The phase function (1), therefore, is expected to give good approximation for randomly oriented spheroids. The effect of size distribution is also similar. Essentially, a polydispersion also washes out the oscillations in the angular variation of the phase function. This can be seen, for example, in phase functions shown in Corenette and Shanks [9] for modified gamma distributions of Mie particles for Haze C, Haze M and cloud C1 models and also in the work of Mishchenko [10,11] for randomly oriented polydispersion of spheroids. As a consequence, Eq. (1) may describe the phase function satisfactorily even for larger spheroids. However, when the oscillations are still present, the large spheroid formula (2) or its variant may be employed.

4. Test of new phase functions for infinitely long cylindrical particles

Our next test case is that of the scattering of unpolarized light by aligned infinitely long right circular cylinders. As the scattering problem is now a two-dimensional one, the normalization and
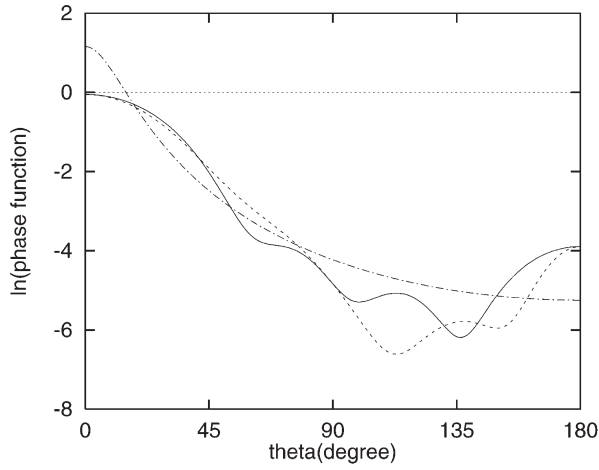
Fig. 5. A comparison of $\Phi_{new}^{ls}(\theta)$ with $\Phi_{ex}(\theta)$ for aligned monodisperse spheroidal particles with $x = 5.0$, $m = 1.5$ and $a/b = 2.0$. Solid line: $\Phi_{ex}(\theta)$; Dashed line: $\Phi_{new}^{ls}(\theta)$ and dash-dot line: $\Phi_{hg}(\theta)$.
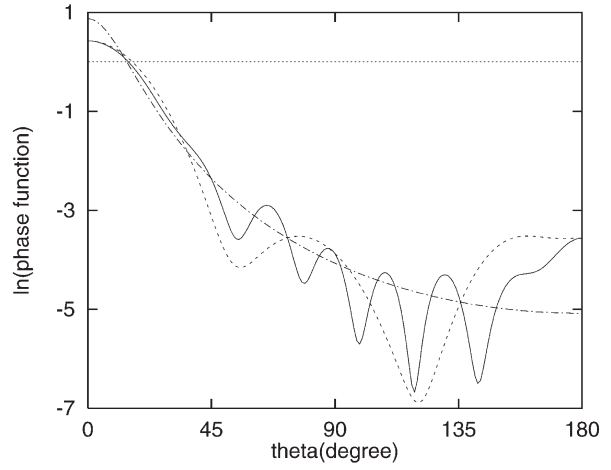
Fig. 6. Same as Fig. 5, but with $x = 10.0$ and $\Phi_{new}^{l}(\theta)$ instead of $\Phi_{new}^{ls}(\theta)$.

Table 1
Values of parameters used in the large particle phase function graphs

Scatterer	x	μ	vk	p	q	s_1	s_2	Formula used
Spheroid								
	5.0	3	−12	6	1	0.00568	0.00535	Φ_{new}^{ls}
	10.0	5	514	8	5	0.000188	0.0000068	Φ_{new}^{l}
Cylinder								
	10.0	28	2818	2	1	0.0080	− 0.000657	Φ_{new}^{l}
	25.0	140	14018	6	1	0.000476	− 0.002629	Φ_{new}^{l}

asymmetry conditions become

$$\int_{0}^{2\pi} \Phi_{new}^{s,l}(\theta)\,d\theta = 1$$

and

$$\int_{0}^{2\pi} \cos\theta\, \Phi_{new}^{s,l}(\theta)\,d\theta = g.$$

This results in the following redefinition of the parameters a_2 and a_4 in Eq. (1):

$$a_2 = \frac{\Phi_{ex}(0) + \Phi_{ex}(\pi)}{2} - a_0 - a_4$$

and

$$a_4 = 4a_0 + 2[\Phi_{ex}(0) + \Phi_{ex}(\pi)] - \frac{4}{\pi},$$

in respect of the Φ_{new}^s for cylinders. The other three parameters occurring in the expression for Φ_{new}^s, namely, a_0, a_1 and a_3 remain unaltered.

For the large radii case given by (2), the cylindrical geometry analogues of (3) and (4), respectively, are given by

$$c_{pq}\Phi_{ex}(\pi/2) + f(\mu)\Phi_{ex}(0) + f(k)\Phi_{ex}(\pi) + \frac{s_1}{8} = \frac{1}{2\pi} \tag{6}$$

and

$$d_{pq}\Phi_{ex}(\pi/2) + f(v+1)\Phi_{ex}(0) - f(k+1)\Phi_{ex}(\pi) + \frac{s_2}{16} = \frac{g}{2\pi}, \tag{7}$$

where

$$c_{pq} = \frac{1}{2\pi}\int_0^{2\pi}(1 + \cos\theta)^p(1 - \cos\theta)^q \, d\theta = \frac{(2p)!(2q)!}{2^{p+q}p!q!(p+q)!},$$

$$d_{pq} = \frac{1}{2\pi}\int_0^{2\pi}\cos\theta(1 + \cos\theta)^p(1 - \cos\theta)^q \, d\theta = \frac{p-q}{p+q+1}c_{pq},$$

and the function $f(n)$ is

$$f(n) = \frac{1}{4\pi}\int_0^{2\pi}\cos^{2n}\theta \, d\theta = \frac{2n!}{2^{2n+1}(n!)^2}$$

for positive integer n. Here, μ, v, p, q and k are all integers.

Finally, we observe that it is also possible to define a Henyey–Greenstein-type phase function ($\tilde{\Phi}_{hg}$) for two-dimensional geometry as (see the appendix)

$$\tilde{\Phi}_{hg} = \frac{1 - g^2}{2\pi(1 + g^2 - 2g\cos\theta)}, \tag{8}$$

which may be noted to yield correct normalization and asymmetry parameter for cylindrical geometry.

The numerical comparisons of Φ_{new}^s with exact phase functions have been performed in the x range 0.1–2.0. Here $x = 2\pi a/\lambda$ with a as the radius of the cylinder. Figs. 7 and 8 show typical comparisons of Φ_{new}^s with Φ_{ex} and $\tilde{\Phi}_{hg}$ for $x = 0.5$ and 1.0, respectively. The refractive index of the cylinders is 1.5. It can be seen that the Φ_{new}^s reproduces the exact results correctly over the entire angular range. In calculating the parameter a_1 the angular interval has been chosen to be $0.1°$. Since the phase function is very smooth at and near $\theta = 90°$ for small particles, a_1 is not very senstive to small changes in the magnitude of the interval. In fact, even when the interval is increased to $1°$ the change in the value of a_1 is negligible. For large diameter cylinders, comparisons have been made in the range $x = 3.0$–50.0. Representative results of comparison of Φ_{new}^l with
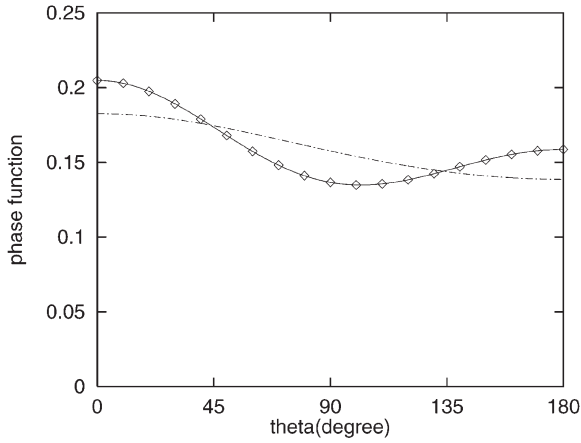
Fig. 7. A comparison of $\Phi_{new}^s(\theta)$ with $\Phi_{ex}(\theta)$ for aligned monodisperse infinitely long cylindrical particles. Here $x = 0.5$ and $m = 1.5$. Solid line: $\Phi_{ex}(\theta)$; Boxes: $\Phi_{new}^s(\theta)$; Dash-dot line: $\tilde{\Phi}_{hg}(\theta)$.
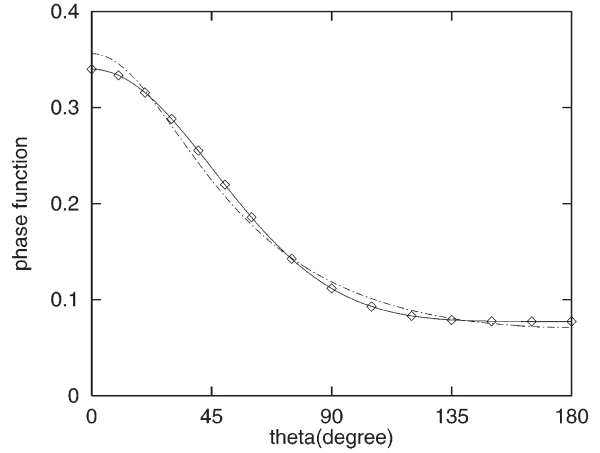
Fig. 8. Same as Fig. 7, but with $x = 1.0$.

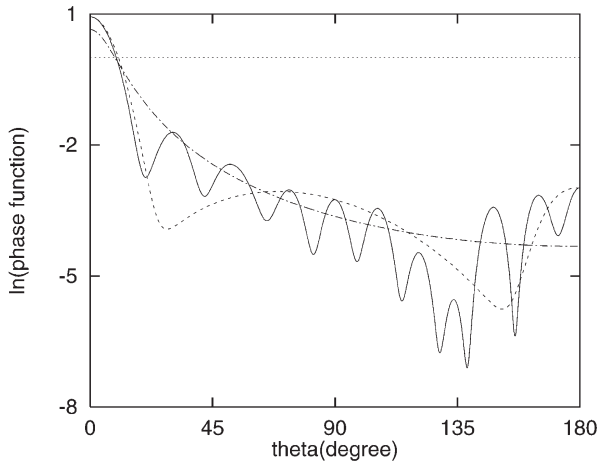Fig. 9. A comparison of $\Phi_{new}^l(\theta)$ with $\Phi_{ex}(\theta)$ for aligned monodisperse infinitely long cylindrical particles with $x = 10.0$ and $m = 1.5$. Solid line: $\Phi_{ex}(\theta)$; Dashed line: $\Phi_{new}^l(\theta)$ and dash-dot line: $\tilde{\Phi}_{hg}(\theta)$.
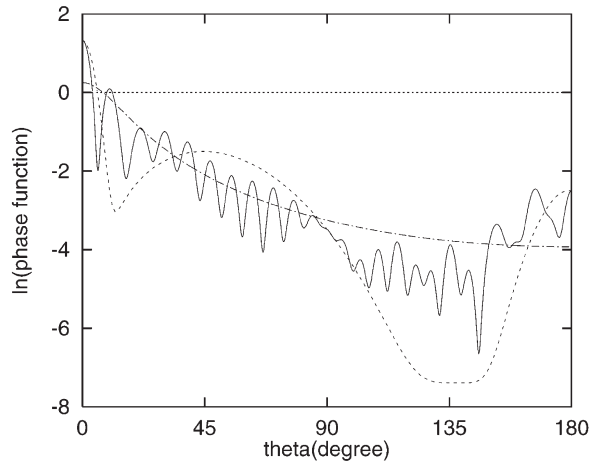
Fig. 10. Same as Fig. 9, but with $x = 25.0$.

Φ_{ex} and $\tilde{\Phi}_{hg}$ are shown for $x = 10.0$ and 25.0 in Figs. 9 and 10, respectively. As in the case of spheres and spheroids, Φ_{new}^l can be seen to be a good representation of the exact phase function for cylinders too. It constitutes significant improvement over $\tilde{\Phi}_{hg}$ in the near forward direction. The exact Results have been obtained employing the computer program given in Barber and Hill [8]. The procedure for obtaining various parameters required as input for parametrizing the phase function is same as described in Section 2. The value of these parameters corresponding to Figs. 9 and 10 are shown in Table 1.

The effect of random orientations and polydispersions for cylinders has been studied by Mishchenko [12] and by Kuik et al. [13]. As expected, random orientations and polydispersions result only in decrease of oscillations in the angular variation of the phase functions. Clearly, our phase functions (1) and (2) are expected to be useful phase functions for such ensembles too.

5. Conclusions

In this paper, we have examined the approximate phase functions, Φ_{new}^{s} and $\Phi_{new}^{l}(\Phi_{new}^{ls})$, designed by us earlier in the context of spherical particles, for scattering of unpolarized light by aligned monodispersions of spheroidal and infinitely long cylindrical particles.

Numerical comparisons of Φ_{new}^{s} with Φ_{ex} show excellent agreement with Φ_{ex} for spheroids as well as infinitely long cylinders. The comparisons clearly demonstrate that Φ_{new}^{s} is capable of reproducing the exact phase function truly and completely at all scattering angles for small nonspherical particles also. Obviously then, it constitutes substantial improvement over all other approximate phase functions. As was shown by us earlier [7], formula (1) leads to a simple analytic expression for the asymmetry parameter and hence provides a simple alternative way of calculating g accurately. The only input needed is the values of the phase function at 0, 90 and 180° and the slope of the phase function at 90°. For large particles, the new phase function $\Phi_{new}^{l}(\Phi_{new}^{ls})$ are found to constitute significant improvement over $\tilde{\Phi}_{hg}$ or Φ_{hg} in the forward lobe. This is important because the dominant part of the phase function indeed comes from this part of the phase function. Outside the forward lobe also the new phase function appears to have an edge over the Henyey–Greenstein phase function.

Although we have restricted our studies in this investigation to monodisperse aligned particles, we note that the approximate phase functions presented here are expected to be useful even for the phase functions relating to polydispersions and nonaligned particles. These factors effectively reduce the oscillations in the angular variation in the phase functions. It, therefore, appears that the phase function given by (1) could be applicable for polydisperse nonaligned nonspherical particles of large sizes too. However, in cases where the oscillations are still significant, one should employ the large particle phase functions.

Having established the accuracy of the new phase functions (1) and (2) for spherical as well as nonspherical monodisperse aligned particles, we now propose, to examine in details the accuracy of these new phase functions for polydisperse and/or nonaligned particles and also to investigate about the gains one may achieve by use of these phase functions in practical solutions of the multiple scattering problems under various physical conditions.

Appendix

The formula for $\tilde{\Phi}_{hg}$ given by Eq. (8) in Section 4 is easily obtained by considering a simple two-parameter empirical expression for the phase function in cylindrical geometry of the form

$$\Phi^{cyl}(\theta) = \frac{1}{a - b\cos\theta} \quad (a > b > 0), \tag{9}$$

where $a > b$ ensures positivity of $\Phi^{cyl}(\theta)$ for all θ. The chosen form of the denominator in (9) also ensures that $\phi^{cyl}(0) > \Phi^{cyl}(180)$. The parameters a and b occuring in $\Phi^{cyl}(\theta)$ are now determined using the following conditions.

(i) $\Phi^{cyl}(\theta)$ is normalized. This condition yields the equation

$$\int_0^{2\pi} \Phi^{cyl}(\theta)\, d\theta = \int_0^{2\pi} \frac{d\theta}{a - b\cos\theta} = \frac{2\pi}{\sqrt{a^2 - b^2}} = 1. \tag{10}$$

(ii) $\Phi^{cyl}(\theta)$ generates the true value of the asymmetry parameter g. This leads to the equation

$$\int_0^{2\pi} \Phi^{cyl}(\theta)\cos\theta\, d\theta = \int_0^{2\pi} \frac{\cos\theta}{a - b\cos\theta} = \frac{a}{b} - \frac{2\pi}{b} = g. \tag{11}$$

Using Eqs. (10) and (11), we solve for a and b to obtain

$$a = 2\pi\frac{1 + g^2}{1 - g^2}, \qquad b = 2\pi\frac{2g}{1 - g^2}.$$

Substituting these values for a and b in (9), we have finally

$$\Phi^{cyl}(\theta) = \frac{1 - g^2}{2\pi(1 + g^2 - 2g\cos\theta)}.$$

This phase function looks very similar to the Henyey–Greenstein phase function given by Eq. (5). For this reason, we have addressed to $\Phi^{cyl}(\theta)$ as $\tilde{\Phi}_{hg}$, the Henyey–Greenstein-type phase function.

References

[1] Henyey LC, Greenstein J. Astrophys J 1941;93:70.
[2] Chu CM, Churchill SW. J Opt Soc Am 1955;45:958.
[3] Irvine WM. Astrophys J 1965;4:1563.
[4] Kattawar GW. JQSRT 1975;15:839.
[5] Reynolds LA, McCormick NJ. J Opt Soc Am 1980;70A:1206.
[6] Liu P. Phys Med Biol 1994;39:1025.
[7] Sharma SK, Roy AK, Somerford DJ. JQSRT 1998;60:1001.
[8] Barber PW, Hill SC. Light scattering by particles: computational methods. Singapore: World Scientific, 1990.
[9] Cornette WM, Shanks JG. Appl Opt 1992;31:3152.
[10] Mishchenko MI. Appl Opt 1993;32:4652.
[11] Mishchenko MI, Travis LD, Kahn RA, West RA. J Geophys Res 1997;102:16 831.
[12] Mishchenko MI, Travis LD, Macke A. Appl Opt 1996;35:4927.
[13] Kuik F, de Haan JF, Hovenier JW. Appl Opt 1994;33:4906.